

Semi-soft Nematic Elastomers and Nematics in Crossed Electric and Magnetic Fields

Fangfu Ye,¹ Ranjan Mukhopadhyay,² Olaf Stenull,³ and T. C. Lubensky¹

¹*Department of Physics and Astronomy, University of Pennsylvania, Philadelphia, PA 19104, USA*

²*Department of Physics, Clark University, Worcester, MA 01610, USA*

³*Fachbereich Physik, Universität Duisburg-Essen, Lotharstr. 1, 47048 Duisburg, Germany*

(Dated: August 24, 2021)

Nematic elastomers with a locked-in anisotropy direction exhibit semi-soft elastic response characterized by a plateau in the stress-strain curve in which stress does not change with strain. We calculate the global phase diagram for a minimal model, which is equivalent to one describing a nematic in crossed electric and magnetic fields, and show that semi-soft behavior is associated with a broken symmetry biaxial phase and that it persists well into the supercritical regime. We also consider generalizations beyond the minimal model and find similar results.

PACS numbers: PACS: 61.30.Vx, 61.41.+e, 64.70.Md

Nematic elastomers (NEs) [1] are remarkable materials that combine the elastic properties of rubber with the orientational properties of nematic liquid crystals. An ideal uniaxial nematic elastomer is produced when an isotropic rubber, formed by crosslinking a polymer with nematogenic mesogens, undergoes a transition to the nematic phase in which it spontaneously stretches along one direction (the z -direction) and contracts along the other two while its nematic mesogens align on average along the stretch direction. This ideal nematic phase exhibits soft-elasticity [2, 3] – a consequence of Goldstone modes arising from the breaking of the continuous rotational symmetry of the isotropic phase [4]. Soft elasticity is characterized by the vanishing of the elastic modulus C_5 measuring the energy associated with shears u_{xz} and u_{yz} in planes containing the anisotropy axis and by a stress-strain curve for strains u_{xx} (or u_{yy}) and stresses σ_{xx} (or σ_{yy}) perpendicular to the anisotropy axis in which strains up to a critical value are produced at zero stress as shown in Fig. 1(a).

Monodomain samples cannot be produced without locking in a preferred anisotropy direction, usually by the Küpfer-Finkelmann (KF) procedure [5] in which a first crosslinking in the absence of uniaxial stress is followed by second one with stress. This process introduces a mechanical aligning field h , analogous to an external electric or magnetic field, and lifts the value of the elastic modulus C_5 from zero. Thus, nematic elastomers prepared in this way are simply uniaxial solids with a linear stress strain relation at small strain. For fields h that are not too large, however, they are predicted to exhibit semi-soft elasticity [1, 6] in which the nonlinear stress-strain curve exhibits a flat plateau at finite stress as shown in Fig. 1(a). Measured stress-strain curves in appropriately prepared samples unambiguously exhibit the characteristic semi-soft plateau [7, 8].

The Goldstone argument for soft response predicts $C_5 = 0$ in the nematic phase, making reasonable conjectures that C_5 should remain small at finite h when semi-soft response is expected and that semi-soft response

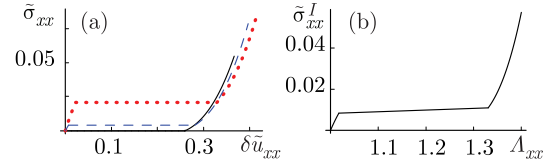


FIG. 1: (a): Soft (full line) and semi-soft (dashed and dotted lines) stress-strain curves at $\tilde{r} = 0.08$ with $\tilde{h} = 0, 0.8\tilde{h}_c, 4\tilde{h}_c$, respectively. (b) Semi-soft curve of $\tilde{\sigma}_{xx}^I$ as a function of A_{xx} at $\tilde{r} = 0.08$ and $\tilde{h} = 2\tilde{h}_c$, where we have set $v = w$.

might not exist at all in the supercritical regime [9] beyond the mechanical critical point (with $h = h_c$) terminating the paranematic(PN)-nematic(N) coexistence line [10]. There is now strong evidence [11, 12] that samples prepared with the KF technique are supercritical. In addition, C_5 measured in linearized rheological experiments is not particularly small [12]. These results have caused some to doubt the interpretation of the measured stress-strain plateau in terms of semi-soft response [13].

The purpose of this paper is to clarify the nature of semi-soft response. We consider the simplest or minimal model, which is formally equivalent to the Maier-Saupe-de-Gennes model [14] for nematic liquid crystals, that exhibits this response. We derive the global mean-field phase diagram [Fig. 2] for this model. We show that semi-soft response is associated with biaxial phases that spontaneously break rotational symmetry, and we unambiguously establish that semi-soft response exists well into the supercritical regime. Figure 1 shows calculated stress-strain curves for $h = 0.8h_c$ and $h = 4h_c$ that clearly exhibit semi-soft behavior both for $h < h_c$ and in the supercritical regime with $h > h_c$. Our minimal model provides a robust description of semi-soft response. We will, however, briefly discuss changes in this response that extensions of the minimal model can bring about.

An elastomer is characterized by an equilibrium reference configuration, which we refer to as a reference space S_R , with mass points at positions \mathbf{x} . Upon dis-

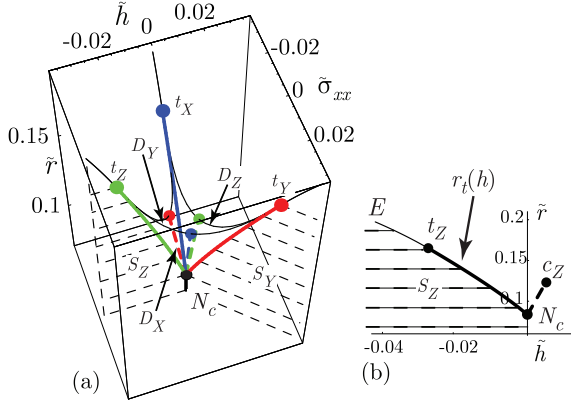


FIG. 2: Phase diagrams (a) in the \tilde{h} - $\tilde{\sigma}_{xx}$ - \tilde{r} space showing the S_Y and S_Z (S_X hidden) CC and the D_X , D_Y , and D_Z DC surfaces along with the tricritical points t_X , t_Y , t_Z and (b) in the \tilde{r} - \tilde{h} plane ($\tilde{\sigma}_{xx} = 0$) showing the first-order uniaxial PN - N coexistence line $N_c c_Z$, the mechanical critical point c_Z , and the S_Z surface terminated by the line $\tilde{r}_t(\tilde{h})$ with respective first- and second-order segments $N_c t_Z$ and $t_Z E$ meeting at the tricritical point t_Z .

tortion of the elastomer, points \mathbf{x} are mapped to points $\mathbf{R}(\mathbf{x}) \equiv \mathbf{x} + \mathbf{u}(\mathbf{x})$ in a target space S_T , where $\mathbf{u}(\mathbf{x})$ is the displacement variable. Elastic distortions that vary slowly on scales set by the distance between crosslinks are described by the Cauchy deformation tensor $\mathbf{\Lambda}$ with components $\Lambda_{ij} = \partial R_i / \partial x_j$. The usual Lagrangian strain tensor is then $\mathbf{u} = (\mathbf{\Lambda}^T \cdot \mathbf{\Lambda} - \delta) / 2$, where δ is the unit matrix. The orientational properties of nematic mesogens in the elastomer are measured by the Maier-Saupe nematic tensor \mathbf{Q} .

A complete theory for nematic elastomers should treat both $\mathbf{\Lambda}$ and \mathbf{Q} and couplings between them. However, effective theories, obtained by integrating out Q_{ij} , that depend only on \mathbf{u} provide a full description of the mechanical properties of NEs [4, 15]. In such theories, strains measure distortions relative to an isotropic reference state, and the elastic free-energy density $f(\mathbf{u})$ consists of an isotropic part $f_{\text{iso}}(\mathbf{u})$ and an anisotropic part $f_{\text{ani}}(\mathbf{u}, h)$ arising from the imprinting process [5]. Equilibrium in the presence of an external second Piola-Kirchhoff (PK) stress σ_{xx} is determined by minimization over \mathbf{u} of the Gibbs free energy density $g(\mathbf{u}, h, \sigma_{xx}, r) = f_{\text{iso}}(\mathbf{u}, r) + f_{\text{ani}}(\mathbf{u}, h) + f_{\text{ext}}(\mathbf{u}, \sigma_{xx})$, where $f_{\text{ext}}(\mathbf{u}, \sigma_{xx},) = -\sigma_{xx} u_{xx}$. In equilibrium the second PK stress satisfies $\sigma_{ij} = \partial f / \partial u_{ij}$. We will return later to the engineering or first PK stress tensor $\sigma_{ij}^I = \partial f / \partial \Lambda_{ij} = \Lambda_{ik} \sigma_{kj}$.

We now define our minimal model. First, we impose the constraint $\text{Tr} \mathbf{u} = 0$, enforcing incompressibility at small but not large \mathbf{u} , rather than the full nonlinear incompressibility constraint $\det \mathbf{\Lambda} = [\det(\delta + 2\mathbf{u})]^{1/2} = 1$ that more correctly describes NEs, whose bulk moduli are generally orders of magnitude larger than their shear moduli. Our theory thus depends only on the symmetric-

traceless components of \mathbf{u} : $\phi_{ij} = u_{ij} - \frac{1}{3} \delta_{ij} u_{kk}$, and $f_{\text{ext}} = -\sigma_{xx} \phi_{xx}$. Second, we use the simplest anisotropy energy: $f_{\text{ani}} = -h u_{zz} \rightarrow -h \phi_{zz}$ that favors stretching along the z axis. Thus, our theory is formally equivalent to that for a nematic liquid crystal in crossed electric and magnetic fields, $\mathbf{E} = E \mathbf{e}_z$ and $\mathbf{H} = H \mathbf{e}_x$, in which $\phi_{ij} \leftrightarrow Q_{ij}$, $h \leftrightarrow \frac{1}{2} \Delta \epsilon E^2$, and $\sigma_{xx} \leftrightarrow \frac{1}{2} \chi_a H^2$, where $\Delta \epsilon$ and χ_a are, respectively, the anisotropic parts of the dielectric tensor and the magnetic susceptibility, and \mathbf{e}_a , $a = x, y, z$, are unit vectors along direction a . Finally, we choose the Landau-de-Gennes form [14] for f_{iso} :

$$f_{\text{iso}}(\phi, r) = \frac{1}{2} r \text{Tr} \phi^2 - w \text{Tr} \phi^3 + v (\text{Tr} \phi^2)^2, \quad (1)$$

where we assume $w > 0$ and where $r = a(T - T^*)$ with T the temperature and T^* the temperature at the metastability limit of the PN phase. In the isotropic phase with $\phi = 0$, $r = 2\mu$, where μ is the T -dependent shear modulus. We will often express quantities in reduced form: $\tilde{u}_{ij} = (v/w) u_{ij}$, $\tilde{r} = r v / w^2$, $\tilde{h} = h v^2 / w^3$, $\tilde{\sigma}_{ij} = \sigma_{ij} v^2 / w^3$, $\tilde{C}_5 = C_5 v / w^2$, and similarly for other elastic moduli.

We begin our analysis of the global phase diagram [16] with the $\sigma_{xx} = 0$ plane, which we will refer to as the Z -plane because the anisotropy field h favors uniaxial order along the z -axis. The $h \geq 0$ half of this plane exhibits the familiar nematic clearing point N_c at $(\tilde{r}_N, \tilde{h}_N) = (\frac{1}{12}, 0)$ and the PN - N coexistence line terminating at the mechanical critical point $(\tilde{r}_c, \tilde{h}_c) = (\frac{1}{8}, \frac{1}{192})$. Throughout the $h > 0$ half-plane, there is prolate uniaxial order with $\phi_{ij} = S(n_i n_j - \frac{1}{3} \delta_{ij})$ with $S > 0$ and the Frank director \mathbf{n} along \mathbf{e}_z . In the N phase at $h = 0$ and $r < r_N$, \mathbf{n} can point anywhere on the unit sphere. Negative h induces oblate rather than prolate uniaxial order along \mathbf{e}_z and $S = -S' < 0$ at high temperature. When $h < 0$ is turned on for $r < r_N$ at which nematic order exists at $h = 0$, \mathbf{n} aligns in the two-dimensional xy -plane. This creates a biaxial environment and biaxial rather than uniaxial order. Since \mathbf{n} can point anywhere in the xy -plane, the biaxial state at $h < 0$ exhibits a spontaneously broken symmetry. There must be a transition along a line $r = r_t(h)$ between the high-temperature oblate uniaxial state and the low-temperature biaxial state, which exists throughout the S_Z surface shown in Fig. 2. This transition is first order at small $|h|$ because the PN - N transition is first order at $h = 0$ and second order at larger $|h|$, and there is a tricritical point [17] t_Z at $(\tilde{r}_t, \tilde{h}_t) = (\frac{21}{128}, -\frac{27}{1024})$ separating the two behaviors as shown in Fig. 2(b). A continuum of biaxial states coexist on S_Z . We will refer to such surfaces as CC surfaces and ones on which a discrete set of states coexist as DC surfaces.

The full phase diagram reflects the symmetries of g . The x - and z -directions are equivalent in f_{iso} , and the $\sigma_{xx} = 0$ and the $h = 0$ planes are symmetry equivalent. These planes are also equivalent (apart from stretching) to the vertical plane with $\sigma_{xx} = h$, but with positive and negative directions interchanged. To see this, we note

that $\phi_{zz} + \phi_{xx} = -\phi_{yy}$ and $h\phi_{zz} + \sigma_{xx}\phi_{xx} = -h\phi_{yy}$ when $h = \sigma_{xx}$. Thus the phase structure of the Z -plane is replicated in the X -plane ($h = 0$) and the Y -plane ($\sigma_{xx} = h$) with respective preferred uniaxial order along \mathbf{e}_x and \mathbf{e}_y , critical points c_X and c_Y , biaxial coexistence surfaces S_X and S_Y , and tricritical points t_X and t_Y .

To fill in the $3D$ phase diagram, we consider perturbations away from the X -, Y -, and Z -planes. Turning on σ_{xx} converts the PN - N coexistence line into a DC surface D_Z , on which two discrete in general biaxial phases coexist. Turning on σ_{xx} near the S_Z surface favors alignment of the biaxial order along \mathbf{e}_x when $\sigma_{xx} > 0$ and along \mathbf{e}_y when $\sigma_{xx} < 0$. Thus σ_{xx} is an ordering field for biaxial order whereas a linear combination of h and σ_{xx} acts as a nonordering field. The topology of the phase diagram near t_Z is that of the Blume-Emery-Griffiths model [18] with DC surfaces D_X and D_Y emerging from the first-order line N_{ctZ} terminating S_Z . The D_X and D_Y surfaces terminate, respectively, on the critical lines N_{ctX} and N_{ctY} in the X - and Y -planes. The surfaces D_X , D_Y , and D_Z form a cone with vertex at N_c .

Before considering the σ_{xx} - u_{xx} stress-strain curve, it is useful to look more closely at elastic response in the vicinity of the Z -plane and the nature of order in the Y -plane. Throughout the $h > 0$ Z -plane, the equilibrium state is prolate uniaxial with order parameter $S = S_0$, and thus strains $u_{zz}^0 = \frac{2}{3}S_0 = -2u_{xx}^0 = -2u_{yy}^0$. We are primarily interested in shears in the xz -plane and the response to an imposed σ_{xx} with no additional stress along z . In this case $\delta u_{zz} = u_{zz} - u_{zz}^0$ will relax to an imposed δu_{xx} , and the free energy of harmonic deviations from equilibrium can be written as $\delta f = \frac{1}{2}C_3(\delta u_{xx})^2 + \frac{1}{2}C_5(\delta u_{xz})^2$. The modulus C_3 gives the slope of σ_{xx} versus δu_{xx} , and C_5 is measured in linearized rheology experiments [12, 19]. C_3 and C_5 are easily calculated as a function of r and h . In reduced units, the ordered pair $(\tilde{C}_3, \tilde{C}_5)$ takes on the value $(\frac{1}{8}, \frac{1}{8})$ just above N_c ($\tilde{r} = \tilde{r}_N^+$), $(\frac{3}{8}, 0)$ just below N_c ($\tilde{r} = \tilde{r}_N^-$), $(0, \frac{1}{12})$ at the critical point, and $(\frac{57}{112}, \frac{1}{12})$ in the supercritical regime at $(\tilde{r}, \tilde{h}) = (\tilde{r}_c, 2\tilde{h}_c)$. We will measure elastic distortions using δu_{ij} rather than the strain u'_{ij} relative to the reference space S'_R defined by the equilibrium configuration at any given T [20].

On the $h > 0$, Y -plane, there is oblate uniaxial order aligned along the y -direction at high T and biaxial order at low T . A convenient representation of the tensor order parameter is

$$\phi = \begin{pmatrix} \frac{1}{3}S' - \eta_1 & 0 & \eta_2 \\ 0 & -\frac{2}{3}S' & 0 \\ \eta_2 & 0 & \frac{1}{3}S' + \eta_1 \end{pmatrix}, \quad (2)$$

where $S' > 0$. The vector $\vec{\eta} \equiv (\eta_1, \eta_2) \equiv \eta(\cos 2\theta, \sin 2\theta)$ is the biaxial order parameter, which is nonzero on the S_Y surface. We define the equilibrium values of S' and η in the biaxial phase to be S'_0 and η_0 , respectively. Energy in this phase is independent of the rotation angle θ . Away from the Y -plane, $f_{\text{ani}} + f_{\text{ext}} =$

$-\frac{1}{3}(h + \sigma_{xx})S' + (\sigma_{xx} - h)\eta_1$. Thus, $\sigma_{xx} < h$ favors $\eta_1 > 0$ and $\sigma_{xx} > h$ favors $\eta_1 < 0$, implying that $\vec{\eta} = (\eta_0, 0)$ (or $\theta = 0$) at $\sigma_{xx} = h^-$ and $\vec{\eta} = (-\eta_0, 0)$ (or $\theta = \frac{\pi}{2}$) at $\sigma_{xx} = h^+$. These considerations imply that the modulus C_5 is zero at $\sigma_{xx} = h^\pm$ because $C_5 = \partial^2 f / \partial u_{xz}^2 |_{u_{xz} \rightarrow 0} = (2\eta_0)^{-2} \partial^2 f / \partial \theta^2 |_{\theta \rightarrow 0} = 0$.

We can now construct the σ_{xx} - u_{xx} stress-strain curves. At $\sigma_{xx} = 0$, $u_{xx} = u_{xx}^0$; as σ_{xx} is increased from zero, δu_{xx} grows with initial slope $1/C_3$ until $\sigma_{xx} = h^-$ at which point, $\delta u_{xx} = \frac{1}{3}S'_0 - u_{xx}^0 - \eta_0$. At $\sigma_{xx} = h$, further increase of δu_{xx} to a maximum of $\frac{1}{3}S'_0 - u_{xx}^0 + \eta_0$ produces a zero-energy rotation of $\vec{\eta}$ to yield $\delta u_{xx} = \frac{1}{3}S'_0 - u_{xx}^0 - \eta_0 \cos 2\theta$ and a nonzero shear $u_{xz} = \eta_2 = \eta_0 \sin 2\theta$. The growth of η_2 from zero is induced by the vanishing of C_5 at $\sigma_{xx} = h^\pm$ and its becoming negative for $|\eta_1| < \eta_0$. Thus, the characteristic semi-soft plateau is a consequence of C_5 's vanishing at $\sigma_{xx} = h$ and not at $\sigma_{xx} = 0$. Measurements of C_5 at $\sigma_{xx} = 0$ do not provide information about what happens at $\sigma_{xx} = h$. For $\sigma_{xx} > h$, δu_{xx} again grows with σ_{xx} . Figure 1 shows stress-strain curves for different values of \tilde{h} . Thus, semi-soft response is associated with the S_Y surface, which exists at r and h well into the supercritical regime.

A Ward identity provides a rigorous basis for the above picture beyond mean-field theory. $f_{\text{iso}}(\mathbf{u})$ is invariant under rotations of \mathbf{u} , i.e., under $\mathbf{u} \rightarrow \mathbf{U}\mathbf{u}\mathbf{U}^{-1}$ where \mathbf{U} is any rotation matrix. Thus if $f_{\text{ani}} = -\text{Tr}\mathbf{h}\mathbf{u}$, where $h_{ij} = h\epsilon_{z i}e_{z j}$, $f(\mathbf{U}\mathbf{u}\mathbf{U}^{-1}) = f_{\text{iso}}(\mathbf{u}) - \text{Tr}\mathbf{h}\mathbf{U}\mathbf{u}\mathbf{U}^{-1}$, for any \mathbf{U} , including one describing an infinitesimal rotation by γ about the y -axis with components $U_{ij} = \delta_{ij} + \epsilon_{yij}\gamma$, where ϵ_{ijk} is the Levi-Civita anti-symmetric tensor. Equating the term linear in γ in $f(\mathbf{U}\mathbf{u}\mathbf{U}^{-1})$ to that of $\text{Tr}\mathbf{h}\mathbf{U}\mathbf{u}\mathbf{U}^{-1}$ yields the Ward identity

$$\sigma_{xz}(u_{zz} - u_{xx}) = (\sigma_{zz} + h - \sigma_{xx})u_{xz}, \quad (3)$$

where $\sigma_{ij} = \partial f / \partial u_{ij}$. This identity applies for any f_{iso} , including ones with no compressibility constraint, so long as f_{ani} is linear in \mathbf{u} . In the semi-soft geometry $\sigma_{xz} = \sigma_{zz} = 0$ but $\sigma_{xx} > 0$. Thus, either $u_{xz} = 0$ or $\sigma_{xx} = h$ for any nonzero u_{xz} . Equation (3) also gives $C_5 = \sigma_{xz}/u_{xz}|_{u_{xz} \rightarrow 0} = (h - \sigma_{xx})/(u_{zz} - u_{xx}) = |h - \sigma_{xx}|/2\eta_0$ implying that $C_5 \rightarrow 0$ as $\sigma_{xx} \rightarrow h^\pm$ as long as $\eta_0 \neq 0$.

We have focussed on the effects of an external second PK stress σ_{xx} . In physical experiments, the first PK (engineering) stress, $\sigma_{ij}^I = \partial f / \partial \Lambda_{ij} = \Lambda_{ik}\sigma_{kj}$, or the Cauchy stress, $\sigma_{ij}^C = \sigma_{ik}^I \Lambda_{kj}^T / \det \mathbf{\Lambda}$ (as in [1, 8]), is externally controlled. The σ_{xx}^I - Λ_{xx} stress-strain curve is easily obtained from the σ_{xx} - u_{xx} curve using $\sigma_{xx}^I = \Lambda_{xx}\sigma_{xx}$ and $\Lambda_{xx} = \sqrt{1 + 2u_{xx}}$. These two curves are similar, but the flat plateau in the σ_{xx}^I - Λ_{xx} curve rises linearly with Λ_{xx} as shown in Fig. 1(b), and there is a unique value of Λ_{xx} for each value of σ_{xx}^I . Thus, the S_Y surface in the r - h - σ_{xx} phase diagram would open into a finite volume biaxial region in the r - h - σ_{xx}^I phase diagram with a particular value of $\vec{\eta}$ at each point in it. The phase diagram in the h - σ_{xx}^I

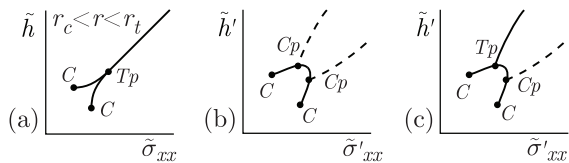


FIG. 3: Schematic phase diagrams in the h (or h')-stress plane. The points Tp , C and Cp are, respectively, triple points, liquid-gas-like critical points, and critical endpoints. (a) Diagrams for the minimal model, where all transitions are first order; (b) and (c) Phase diagrams for more general f_{ani} or f_{ext} in which the first-order line from S_Y is replaced by a surface terminated by two second-order (dashed) lines or one first-order line and one second-order line. h' and σ'_{xx} are, respectively, the generalized aligning field and generalized external stress resulting from the more general f_{ani} or f_{ext} .

plane for $r_c < r < r_t$ is similar to that in Fig. 3(b).

We have ignored boundary conditions and random stress, both of which can modify stress-strain curves. When Frank elastic energies are ignored, detailed calculations of domain structure induced by boundary conditions reproduce soft and semi-soft response [21]. Small isotropic randomness appears not to affect soft response, but large randomness does [22]. Our approach should serve as a basis for further study of randomness.

We can now consider modifications of the minimal model. A simple modification is to replace the constraint $\text{Tr} \mathbf{u} = 0$ with the real volume constraint $\det \mathbf{\Lambda} = 1$. This replacement does not change the validity of the Ward identity and the resulting phase diagram has the same structure as that for $\text{Tr} \mathbf{u} = 0$ but with different boundaries for the CC and DC surfaces. In particular, the mechanical critical point is at $(\tilde{r}_c, \tilde{h}_c) = (0.1279, 0.0052)$ and the tricritical point is at $(\tilde{r}_t, \tilde{h}_t) = (0.1900, 0.0247)$. Other modifications of the minimal model replace f_{ani} with nonlinear functions of u_{zz} . Modifications of this kind can spread the CC surface S_Y into a finite volume or convert it to a DC surface, as shown in Fig. 3. If $f_{\text{ani}} = -hu_{zz}^2$, two states coexist, whereas with other forms such as might arise in a hexagonal lattice, three or more discrete states might coexist. When S_Y is a DC surface, rather than exhibiting a homogeneous rotation of the biaxial order parameter (if boundary conditions are ignored) in response to an imposed u_{xx} , samples will break up into discrete domains of the allowed states. In other words, their response to external stress will be martensitic [23] rather than semi-soft.

The neo-classical model [24] can also be discussed in our language. The free energy of this model is a function of $\mathbf{\Lambda}$ and \mathbf{Q} . It consists of an isotropic part, invariant under simultaneous rotations of $\mathbf{\Lambda}$ and \mathbf{Q} in the target space and under rotations of $\mathbf{\Lambda}$ in the reference space, and a semi-soft anisotropic energy [6], which is effectively

nonlinear in the strain, that breaks rotational symmetry in the reference space. The phase diagram of this model is similar to that of the minimal model in the space of r - h - σ_{xx}^I . In it, semi-soft behavior also persists above the mechanical critical point [25].

In summary, we determined the complete phase diagram of nematic elastomers subject to an internal aligning field and a perpendicular external stress. Our results underscore the validity of semi-softness in the interpretation of their remarkable stress-strain curves.

This work was supported by NSF grant DMR 0404570 and the NSF MRSEC under DMR 05-20020.

-
- [1] M. Warner and E. M. Terentjev, *Liquid Crystal Elastomers* (Oxford University Press, Oxford, 2003).
 - [2] M. Warner, P. Bladon, and E. M. Terentjev, *J. Phys. II (France)* **4**, 93 (1994).
 - [3] P. D. Olmsted, *J. Phys. II (France)* **4**, 2215 (1994).
 - [4] L. Golubović and T. C. Lubensky, *Phys. Rev. Lett.* **63**, 1082 (1989).
 - [5] J. Küpfer and H. Finkelmann, *Makromol. Chem. Rapid Commun.* **12**, 717 (1991).
 - [6] G. Verway and M. Warner, *Macromolecules* **28**, 4303 (1995).
 - [7] J. Küpfer and H. Finkelmann, *Macromol. Chem. Phys.* **195**, 1353 (1994).
 - [8] M. Warner, *J. Mech. Phys. of Solids* **47**, 1355 (1999).
 - [9] O. Stenull and T. C. Lubensky, *Eur. Phys. J. E* **14**, 333 (2004).
 - [10] P. de Gennes, *C.R. Acad. Sci. Ser. B* **281**, 101 (1975).
 - [11] A. Lebar *et al.*, *Phys. Rev. Lett.* **94**, 197801 (2005).
 - [12] D. Rogez *et al.*, *Eur. Phys. J. E* **20**, 369 (2006).
 - [13] H. R. Brand, H. Pleiner, and P. Martinoty, *Soft Matter* **2**, 182 (2006).
 - [14] P. de Gennes and J. Prost, *The Physics of Liquid Crystals* (Oxford University Press, Oxford, 1993).
 - [15] T. C. Lubensky *et al.*, *Phys. Rev. E* **66**, 031704 (2002).
 - [16] B. J. Frisken, B. Bergersen, and P. Palfy-Muhoray, *Mol. Cryst. Liq. Cryst.* **148**, 45 (1987).
 - [17] C.-P. Fan and M. J. Stephen, *Phys. Rev. Lett.* **25**, 500 (1970); R. G. Priest, *Phys. Lett.* **47A**, 475 (1974).
 - [18] M. Blume, V. Emery, and R. Griffiths, *Phys. Rev. A* **4**, 1071 (1971).
 - [19] A. Hotta and E. M. Terentjev, *Eur. Phys. J. E* **10**, 291 (2003); E. M. Terentjev, *et al.*, *Phil. Trans. R. Soc. Lond. A* **361**, 653 (2003).
 - [20] The deformation tensor of the anisotropic equilibrium state at temperature T relative to S_R is $\mathbf{\Lambda}_0$. The strain and stress relative to S'_R are, respectively, $\mathbf{u}' = (\mathbf{\Lambda}_0^T)^{-1} \delta \mathbf{u} (\mathbf{\Lambda}_0)^{-1}$ and $\boldsymbol{\sigma}' = (\det \mathbf{\Lambda}_0)^{-1} \mathbf{\Lambda}_0 \boldsymbol{\sigma} \mathbf{\Lambda}_0^T$.
 - [21] S. Conti, A. DeSimone, and G. Dolzmann, *J. Mech. Phys. of Solids* **50**, 1431 (2002); *Phys. Rev. E* **66**, 061710 (2002).
 - [22] N. Uchida, *Phys. Rev. E* **62**, 5119 (2000).
 - [23] K. Bhattacharya, *Microstructure of Martensite* (Oxford University Press, New York, 2003).
 - [24] P. Bladon, E. Terentjev, and M. Warner, *J. Phys. II (France)* **4**, 75 (1994).
 - [25] F. Ye and T. C. Lubensky (unpublished).